Mon. Not. R. Astron. Soc. **000**, 1–?? (2005) Printed 11 June 2018 (MN LATEX style file v1.4)

Cluster AgeS Experiment (CASE): SX Phe stars from the globular cluster ω Centauri

A. Olech[1], W.A. Dziembowski[2,1], A.A. Pamyatnykh[1,3], J. Kaluzny[1], W. Pych[1], A. Schwarzenberg-Czerny[1,4] and I.B. Thompson[5]

[1] *Nicolaus Copernicus Astronomical Center, ul. Bartycka 18, 00-716 Warsaw, Poland (olech,wd,alosza,jka,pych,alex@camk.edu.pl)*
[2] *Warsaw University Observatory, Al. Ujazdowskie 4, 00-487 Warszawa, Poland*
[3] *Institute of Astronomy, Russian Academy of Sciences, Pyatnitskaya Str. 48, 109017 Moscow, Russia*
[4] *Adam Mickiewicz University Observatory, ul. Słoneczna 36, 60-286 Poznan, Poland*
[5] *Carnegie Institution of Washington, 813 Santa Barbara Street, Pasadena,CA 91101, USA (ian@ociw.edu)*

Accepted .... Received .... in original form ....

ABSTRACT

We present an analysis and interpretation of oscillation spectra for all 69 SX Phoenicis stars discovered in the field of the cluster. For most of the stars we have reliable absolute magnitudes and colors. Except of one, or perhaps two, objects, the stars are cluster members. Their pulsational behaviour is very diversified. Multiperiodic variability with at least part of the excited modes being nonradial is most common but there are also many cases of high amplitude, presumably radial mode, pulsators. In a number of such cases we have evidence for two radial modes being excited. Parameters of radial mode pulsators are in most cases consistent with standard evolutionary models for stars in the mass range $0.9 \div 1.15 M_{\odot}$. However, in four cases we have evidence that the masses are significantly lower than expected. Three objects show frequency triplets that may be interpreted in terms of rotational frequency splitting of $\ell = 1$ modes. Implied equatorial velocities of rotation are from 10 to over 100 km/s. Nearly all measured frequencies fall in the ranges predicted for unstable modes. Two cases of low frequency variability are interpreted as being caused by tidal distortion induced by close companions.

Key words: stars: SX Phe - stars: variables – globular clusters: individual: ω Cen

1 INTRODUCTION

SX Phoenicis stars (SXPS) are the Population II short period pulsators, in most respects similar to much more numerous δ Scuti stars, which are the Population I objects. Both types occupy the low luminosity end of the Cepheid instability strip in the H-R diagram. It is not clear whether there are any systematic differences in pulsation properties between the two types. The incidence of high amplitude pulsation once seemed much higher among SXPS but now, with improved cluster photometry, many low amplitude SXPS are being detected (Pych et al. 2001, Mazur et al. 2003, Kaluzny & Thompson 2003, Kaluzny et al. 2004).

What makes SXPS interesting in a wider context is that they are blue straggler stars (BSS) found in a large number in globular and old open clusters. This means that they have unusual life history which is not well understood as it cannot be explained in terms of the standard single star evolution scenario. The problem of BSS origin is being debated for decades. Historically, the first explanation was that the objects are products of evolution of the mass receiving component in close binary systems (McCrea 1964). Later scenarios involving mergers of main sequence stars were mostly considered. The scenarios included mergers of primordial binaries after a gradual decrease of the orbit (e.g. Carney et al. 2001) as well as direct stellar collisions in dense cluster cores (e.g. Lombardi et al. 2002). It is not clear how much imprints of the past evolution should be left in individual BSS. This depends on the efficiency of chemical element and angular momentum mixing - the processes still poorly understood in stellar interior physics. Understanding the origin and internal structure of BSS is a challenging task for stellar evolution theory. The answer is of interest not only for this field but also for globular cluster research. As emphasized by Lombardi & Rasio (2002), collisions and mergers of stars which lead to BSS formation, play an important role in evolution of these systems.

Pulsation data on SXPS are potential sources of accurate constraints on models of BSS. Each measured frequency of an identified oscillation mode is such a constraint. Admittedly, mode identification is difficult unless we have evidence that the excited modes are radial. Double mode radial pulsators seem quite frequent among SXPS. The two accurately measured numbers yield strong constraints on stellar mass and heavy element content in the interior. Data on nonradial mode frequencies could be even more interesting. In particular, determination of the frequency splitting provides certain mean value of the rotation rate in the interior. Furthermore, there are nonradial modes whose frequencies are very sensitive to the extent of the element mixing beyond the convective core boundary. Of great interest in the context of the debated BSS origin is seeking evidence for presence of close companions manifesting themselves through cyclic period variations or tidally induced variability.

What makes SXPS interesting for stellar pulsation theory is the large diversity of their pulsation forms. In a relatively narrow period range, extending from less than half to two hours, we encounter both the multimode low-amplitude pulsation, typical for main sequence dwarfs, and the monomode high-amplitude pulsation, typical for Cepheids. According to linear nonadiabatic calculations, there are many unstable modes in SXPS. However, finite amplitude development of the instability is not understood. This is the most outstanding unsolved problem of the theory. A sample of SXPS with well constrained mean parameters may provide a key information what makes a star to become a dwarf- or a giant-type pulsator.

The globular cluster ω Centauri houses the largest number of SXPS of all systems in our Galaxy (Kaluzny et al. 2004). Having a large number of objects with well determined luminosities is an obvious advantage. The fact that the stars cannot be assumed coeval and of the same chemical composition (Rey et al. 2000) is a complicating factor. The cluster is atypical. Data on SXPS may prove useful in disentangling its evolution.

In the next section we survey observational data on all SXPS in ω Cen which includes frequency analysis. In section 3 we compare mean photometric parameters of SXPS with the corresponding values calculated for standard evolutionary models. We also provide information on pulsation properties of these models based on the linear nonadiabatic analysis. Section 4 is a star by star analysis of individual objects in which we compare their observational properties with theoretical models. In section 5 we summarize our results.

2 PHOTOMETRY

ω Centauri contains the most numerous population of variable stars among globular clusters of the Galaxy (Clement et al. 2001). However until the mid 1990ies there was only one SX Phe-type variable known in the field of the cluster. It was V65, which in fact turned out later to be a foreground star. However, not much later Kaluzny et al. (1996, 1997) reported a discovery of 25 SXPS, most of which must be members of the cluster. Subsequent work done by Kaluzny et al. (2004) increased the number of SXPS in the field of ω Centauri to 69, making it the richest in these variables among all globular clusters of our Galaxy.

Kaluzny et al. (2004) provide extensive photometry for 61 SXPS collected during two years. This photometry contains from 532 to 755 V and over 150 B measurements for each variable. It is an excellent data base for analyzing multimode behavior and extracting information on physical properties of individual objects.

Table 1. Basic properties of SX Phe-type variables in field of ω Cen.

Star	Period	Amp.	$< V >$	$B-V$	M_V	$(B-V)_0$
V65	0.0627235	0.18	14.922	0.361	0.832	0.231
V194	0.0471777	0.51	17.016	0.330	2.926	0.200
V195	0.0654912	0.38	16.780	0.371	2.690	0.241
V196	0.05740	0.23	17.000	-	2.910	-
V197	0.0471210	0.13	16.850	0.546	2.760	0.416
V198	0.0481817	0.15	17.533	0.323	3.483	0.193
V199	0.0622867	0.73	16.689	0.333	2.599	0.203
V200	0.0495210	0.28	16.568	0.541	2.478	0.411
V201	0.05065	0.19	17.200	-	3.110	-
V202	0.04642	0.12	17.170	-	3.080	-
V203	0.04178	0.25	16.750	-	2.660	-
V204	0.0493757	0.40	16.881	0.363	2.791	0.233
V217	0.0532609	0.10	17.038	0.429	2.948	0.299
V218	0.0437393	0.07	17.095	0.330	3.005	0.200
V219	0.0386680	0.08	17.303	0.337	3.213	0.207
V220	0.0528868	0.12	16.986	0.357	2.896	0.227
V221	0.0361336	0.05	16.680	0.451	2.590	0.321
V222	0.03891	0.05	17.310	-	3.220	-
V225	0.0486381	0.22	16.845	0.393	2.755	0.262
V226	0.0378523	0.17	17.299	0.413	3.209	0.283
V227	0.0382255	0.05	17.272	0.397	3.182	0.267
V228	0.0398531	0.08	17.199	0.403	3.109	0.273
V229	0.0375333	0.09	17.407	0.294	3.317	0.164
V230	0.03388	0.03	16.550	-	2.460	-
V231	0.0374845	0.05	17.419	0.341	3.329	0.211
V232	0.03697	0.04	17.590	-	3.500	-
V233	0.0365376	0.10	17.210	0.353	3.120	0.223
V237	0.0656024	0.27	16.861	0.351	2.771	0.221
V238	0.0408004	0.07	17.355	0.349	3.265	0.219
V249	0.0349468	0.10	17.435	0.361	3.345	0.231
V250	0.0406269	0.07	17.433	0.380	3.343	0.250
V252	0.0466226	0.06	17.445	0.405	3.355	0.275
V253	0.0399687	0.11	17.232	0.308	3.142	0.178
V260	0.04626	0.05	17.080	-	2.990	-
NV294	0.01773360	0.02	17.292	0.328	3.202	0.198
NV295	0.01823127	0.01	17.283	0.357	3.193	0.227
NV296	0.02212644	0.03	16.946	0.365	2.856	0.235
NV297	0.03389566	0.02	16.628	0.301	2.538	0.171
NV298	0.0330389	0.08	17.410	0.354	3.320	0.224
NV299	0.0344409	0.04	17.325	0.432	3.235	0.302
NV300	0.0347301	0.02	17.484	0.363	3.394	0.233
NV301	0.0354431	0.03	16.974	0.439	2.884	0.309
NV302	0.0355192	0.04	17.081	0.362	2.991	0.232
NV303	0.0359503	0.01	16.932	0.322	2.842	0.192
NV304	0.0361405	0.03	17.236	0.421	3.146	0.291
NV305	0.0365672	0.04	17.384	0.391	3.294	0.261
NV306	0.0384044	0.06	17.528	0.370	3.438	0.240
NV307	0.0385032	0.07	17.069	0.519	2.979	0.389
NV308	0.0389852	0.05	17.278	0.382	3.188	0.252
NV309	0.0397455	0.04	16.591	0.362	2.501	0.232
NV310	0.0401776	0.02	16.791	0.415	2.701	0.285
NV311	0.0414132	-	-	-	-	-
NV312	0.0433272	0.06	16.394	0.390	2.304	0.26
NV313	0.0418484	0.16	17.678	0.348	3.588	0.218
NV314	0.0421220	0.08	17.086	0.386	2.996	0.256
NV315	0.0422811	0.10	16.392	0.518	2.302	0.388
NV316	0.0424040	0.03	17.326	0.326	3.236	0.196
NV317	0.0426396	0.05	16.968	0.453	2.878	0.323
NV318	0.0437306	0.02	16.799	0.472	2.709	0.342
NV319	0.0489421	0.10	17.239	0.465	3.149	0.335
NV320	0.0471936	0.08	17.294	0.440	3.204	0.310
NV321	0.0474854	0.10	16.409	0.136	2.319	0.006
NV322	0.0479562	0.08	17.096	-	3.006	-
NV323	0.0493547	0.03	16.638	0.436	2.548	0.307
NV324	0.0512944	0.24	16.402	0.297	2.312	0.167
NV325	0.0535445	0.10	16.410	0.501	2.320	0.371
NV326	0.0569058	0.18	17.041	0.401	2.951	0.271
NV327	0.0606414	0.09	16.642	0.274	2.552	0.144
NV328	0.0899030	0.02	17.054	0.598	2.964	0.468

In addition, ω Cen is the first globular cluster for which the CASE project (Thompson et al. 2001) determined the distance. The analysis of photometric and spectroscopic data for an eclipsing binary OGLE GC17 yielded an apparent distance modulus of $(m-M)_V = 14.09 \pm 0.04$ mag (Kaluzny et al. 2002). It is the most precise and reliable distance determination for this cluster and will be used in our work for calculating the absolute magnitudes of SXPS belonging to ω Cen. We will also use the mean color data dereddened with the color excess $E(B-V) = 0.13$ mag (Schlegel, Finkbeiner & Davis, 1998) to place individual objects in the H-R diagram.

The full list of SXPS located in the field of ω Centauri containing main periods, amplitudes, mean magnitudes and

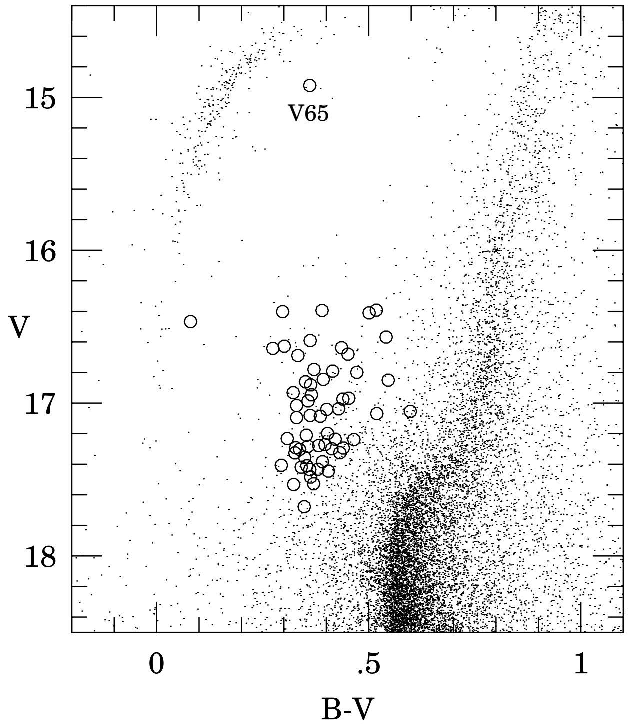

Figure 1. Color-magnitude diagram around blue stragglers region of ω Cen. Points and open circles denote constant stars and SXPS, respectively.

colors is provided in Table 1. Fig. 1 shows color-magnitude diagram around blue stragglers region of ω Cen. Points and open circles denote constant stars and SXPS, respectively. Not all stars in the SXPS region are variables. This is hardly surprising, as we have the same situation in the δ Scuti domain. Presumably these apparently constant objects are very low amplitude pulsators.

3 FREQUENCY ANALYSIS

Many SX Phe stars exhibit multiple periods hence their analysis poses specific challenges. Arguably the most advanced project in terms of both extent of its photometry and multitude of detected periods, the Whole Earth Telescope (WET), employed either the prewhitening *or* synthesis methods in their analysis (Kepler, 1993). From the statistical point of view the two methods correspond to Gauss-Seidel (G-S) and Newton-Raphson (N-R) solutions of the least squares problem (LSQ). On one hand, a current astronomical practice favors the synthesis (N-R) method, employing the covariance matrix with large extra-diagonal coefficients. Presence of close frequencies and/or their combinations in the synthesis method yields near singular normal equations and may produce large near cancelling terms in the solution, creating the $\infty - \infty$ problem and yielding solutions with excess amplitudes. On the other hand, the method recommended to deal with singularity in least squares fitting (LSQ) is by means of the singular value decomposition (SVD, e.g. Press et al., 1986). In the SVD procedure the near

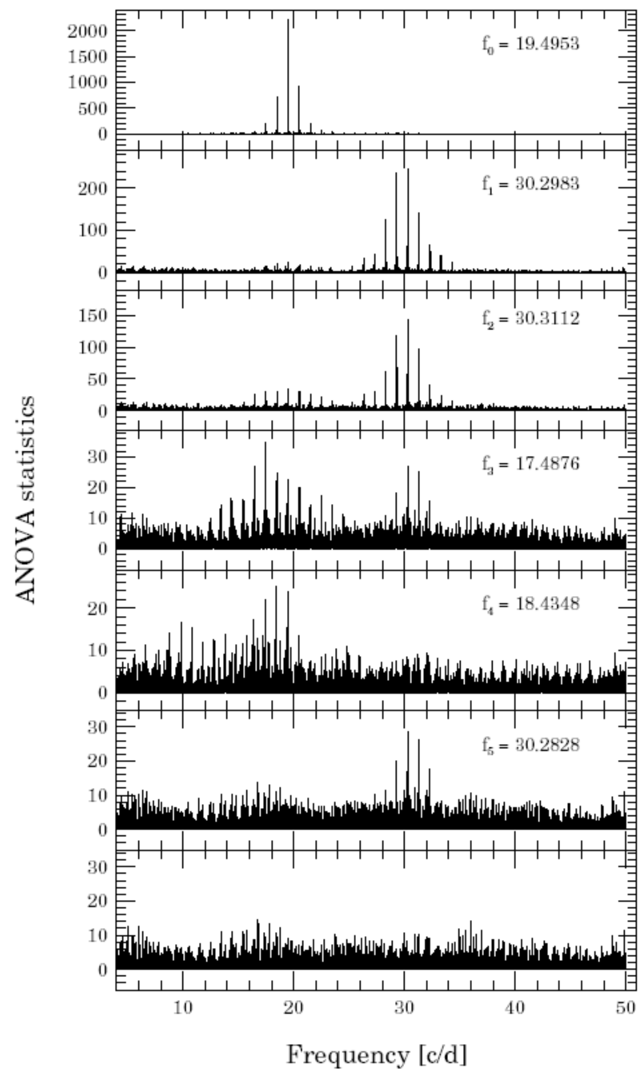

Figure 2. The uppermost panel shows the ANOVA periodogram of the raw light curve of NV324. The panels below show spectra after consecutive prewhitenings.

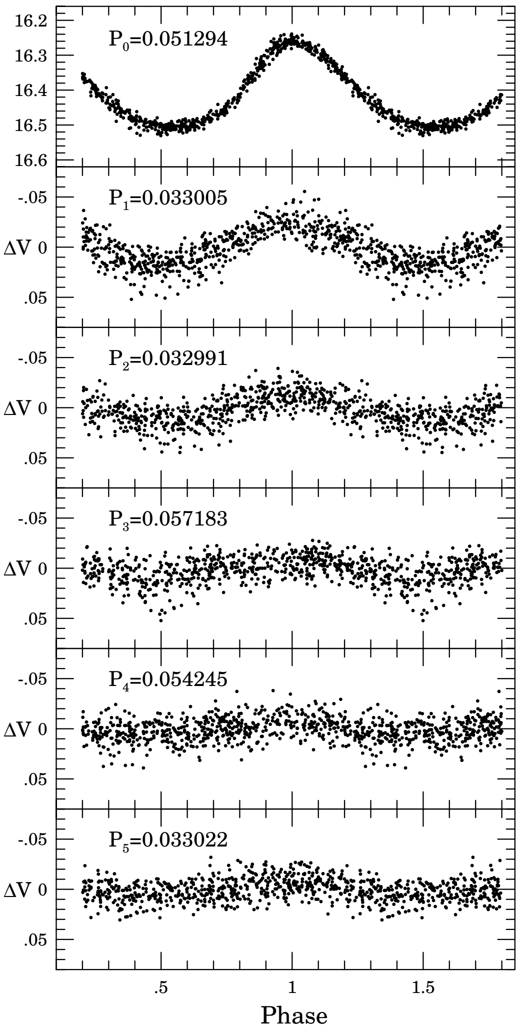

Figure 3. The light curves of NV324 associated with all six periods found. Each light curve, phased with the particular period, was prewhitened with six remaining periods and their harmonics.

singular terms of the covariance matrix are set small, resulting in choice of the solution with minimum norm (minimum amplitudes in the present context). This resembles somewhat the prewhitening method, where implicitly all extra-diagonal terms are set zero (Gray & Desikachary, 1973). We are unaware of any paper comparing merits of the prewhitening and synthesis methods in rigid mathematical (statistical) terms.

We employ the prewhitening and synthesis methods in parallel to analyze our SX Phe light curves. We employed no more than 6 harmonics in prewhitening and in most cases just 2 or 3 harmonics for the f_0 mode and one harmonic for other modes. The values of (fundamental) frequencies were adjusted by nonlinear iterations, their harmonics/combinations were tied to the base frequencies. The resulting frequencies are listed in Table 2. The both methods yielded consistent frequencies for all strong detections, corresponding to the AoV statistics $\Theta > 15$. We observed no adverse effect of reappearance of the frequencies once prewhitened. Ambiguity, if any, arose occasionally due to aliasing and it manifested with equal strength in both the prewhitening and synthesis methods. Such cases are marked in Table 2 with superscript [1].

The novelty in our approach, as compared with WET, is in use of the multi-harmonic AoV periodogram (Schwarzenberg-Czerny, 1996). It employs orthogonal functions and is able to combine power from harmonics (NH=2 harmonics were combined in practice). Importance of use of orthogonal functions in period search was argued by Lomb (1976), Ferraz-Mello (1981), Scargle (1982) and Foster (1994). Advantage in combining harmonics is two-fold: they contribute extra power for the base frequency and at the same time reduce power in the residuals. Any method sensitive to the harmonics (e.g. phase folding and binning and the present case of Fourier fit) is prone to produce sub-harmonics in the periodogram. The subharmonic pose little problem in practice as they are easily identified by tight packing of aliases. There exist exact relations between power in the data, root-mean square (rms) of the residuals and the AoV statistics Θ employed in the present case (e.g. Schwarzenberg-Czerny, 1999). Detection of frequencies poses special case of hypothesis testing in statistics. In our case the detection criterion $\Theta > \Theta_c \equiv 8$ roughly corresponded to mode amplitude exceeding 4 times its standard deviation $A > 4\sigma_A$. Any frequencies near/below that detection limit are deemed unsafe and indicated with superscript [2] in Table 2. The purpose of listing these marginal detections ($15 > \Theta > 8$) is solely to indicate deviations of residuals from pure noise and not to ponder on frequencies.

An example of our results for NV324 is shown in Fig. 2. The panels show ANOVA periodograms (Schwarzenberg-Czerny 1996). The uppermost panel is computed for the original data and reveals the dominant peak with its aliases. The remaining ones are computed for the data after subtraction of all so far identified frequencies and significant combinations of thereof. Fig. 3 shows the light curves of NV324 associated with all six periods found. Each light curve, phased with the particular period, was prewhitened with five remaining periods and their harmonics. Note the asymmetry of the three upper light curves which is typical for pulsating stars. The window function is a concept associated with the power spectrum. Strictly speaking it does not apply for the ANOVA periodogram. However, in Fig. 2 numerous window-like structures are present around principal frequencies.

We refrain here from discussion of amplitudes. On one hand theory results on amplitudes are unreliable (Sect. 4). On the other hand LSQ fits of multifrequency light curves often suffer from large correlation of parameters, indicating large error ellipses despite small variances. We address this problem only indirectly here by relying our analysis on a large sample of stars with very extensive coverage of observations. Application of two independent reduction methods benefitted us in that we checked against any computation errors as well as gained insight into repeatability and reliability of our results.

4 EVOLUTIONARY MODELS AND THEIR OSCILLATION PROPERTIES

Model calculations were made with Warsaw-New Jersey stellar evolution code which is a modern version of Paczyński's (1970) code developed mainly by M. Kozłowski and R.

Table 2. The frequencies found in the light curves of SX Phe variables in the field of ω Cen.

Star	f_0	f_1	f_2	f_3	f_4	f_5	f_6
V65	15.9430(2)	20.2287(1)	21.2182(8)	24.5199(8)	36.1720(8)[1]	-	-
V194	21.1964(1)	27.1633(5)	43.7932(9)	20.7471(6)[1]	22.1462(6)[2]	-	-
V195	15.2692(1)	15.2747(5)	15.2668(6)	-	-	-	-
V197	21.2219(2)	21.3904(5)	21.3129(5)	27.1838(8)	-	-	-
V198	20.7548(3)	-	-	-	-	-	-
V199	16.0548(2)	-	-	-	-	-	-
V200	20.1935(1)	26.5308(5)	-	-	-	-	-
V204	20.2529(1)	26.1552(5)	-	-	-	-	-
V217	18.7755(5)	-	-	-	-	-	-
V218	22.8627(5)	27.0008(6)[1]	43.6865(9)	-	-	-	-
V219	25.8611(6)	26.6204(8)	28.2532(8)	3.2836(3)	-	-	-
V220	18.9083(2)	24.3161(5)	23.8450(7)	-	-	-	-
V221	27.6749(4)	26.9153(5)	32.8848(5)	27.6867(6)	27.6630(9)	-	-
V225	20.5600(2)	26.4145(5)	26.8212(6)	-	-	-	-
V226	26.4185(5)	27.4932(6)	15.4167(5)	25.4523(8)	-	-	-
V227	26.1605(5)	25.4535(9)	28.6334(8)	-	-	-	-
V228	25.0923(5)	24.3732(7)	26.7906(7)[1]	30.0974(9)	-	-	-
V229	26.6429(3)	51.6073(6)	-	-	-	-	-
V231	26.6778(4)	27.1269(6)	27.3509(7)	36.6960(6)[2]	-	-	-
V233	27.3691(2)	2.9205(5)	-	-	-	-	-
V237	15.2433(2)	24.1162(5)	15.2013(8)	-	-	-	-
V238	24.5096(4)	24.1318(8)	25.9960(7)	24.2163(7)[1]	39.5205(7)[2]	-	-
V249	28.6149(4)	35.0000(9)	29.6107(8)	28.6212(8)	-	-	-
V250	24.6142(3)	37.6484(8)	-	-	-	-	-
V252	21.4488(4)	-	-	-	-	-	-
V253	25.0196(5)	25.7372(6)	33.8173(6)	31.1610(7)[1]	-	-	-
NV294	56.3901(6)	28.9864(6)	52.0186(6)	48.4195(6)[1,2]	-	-	-
NV295	54.8509(5)	28.3558(6)	53.9590(6)[1]	31.5356(6)[1]	-	-	-
NV296	45.1948(7)	40.3318(7)[1]	38.6563(7)	42.3111(8)	30.5764(7)[2]	-	-
NV297	29.5022(7)	30.7973(7)	31.8181(7)	30.6969(9)	-	-	-
NV298	30.2674(4)	31.5946(4)	-	-	-	-	-
NV299	29.0352(6)	33.2050(8)	-	-	-	-	-
NV300	29.7935(6)	-	-	-	-	-	-
NV301	28.2141(5)	27.8536(6)	35.3744(7)	51.6717(9)	-	-	-
NV302	28.1538(7)	-	-	-	-	-	-
NV303	27.8162(7)	-	-	-	-	-	-
NV304	27.6698(8)	-	-	-	-	-	-
NV305	27.3469(5)	22.6529(6)	19.0827(7)	15.9932(7)[2]	-	-	-
NV306	26.0387(5)	40.7315(6)	-	-	-	-	-
NV307	25.9719(5)	-	-	-	-	-	-
NV308	25.6507(5)	26.3387(5)	26.0989(7)[1]	49.6777(8)	42.2776(8)[2]	-	-
NV309	25.1601(6)	37.8653(9)	36.0886(8)	25.5930(8)[1]	30.2689(9)[1]	24.5741(9)[2]	38.8636(7)[1]
NV310	24.8894(8)	25.9192(6)	-	-	-	-	-
NV311	24.1469(6)	36.6940(5)	-	-	-	-	-
NV312	23.0802(5)	36.7987(8)	-	-	-	-	-
NV313	23.8958(4)	-	-	-	-	-	-
NV314	23.7405(5)	23.7468(5)	36.4025(6)	-	-	-	-
NV315	23.6513(5)	23.1521(4)	22.8341(6)	34.3549(6)[1]	-	-	
NV316	23.5827(8)	-	-	-	-	-	-
NV317	23.4525(5)	22.7566(6)[1]	24.9835(6)	24.4356(7)	-	-	-
NV318	22.8673(7)	-	-	-	-	-	-
NV319	20.4323(4)	-	-	-	-	-	-
NV320	21.1894(5)	-	-	-	-	-	-
NV321	21.0591(5)	21.5337(7)	20.1156(9)	-	-	-	-
NV322	20.8524(6)	26.8419(6)	20.4605(6)	27.5321(7)[1]	43.3720(6)[1]	25.0637(9)[1]	35.9001(6)[1]
NV323	20.2615(6)	15.7478(6)	-	-	-	-	-
NV324	19.4953(4)	30.2983(7)	30.3112(9)	17.4876(8)	18.4348(9)[1]	30.2828(7)[1]	-
NV325	18.6761(5)	19.0173(7)	19.0683(5)	36.4063(7)	36.3059(6)[1]	34.6931(7)[1]	-
NV326	17.5728(6)	22.5375(6)	-	-	-	-	-
NV327	16.4904(3)	33.2019(9)	-	-	-	-	-
NV328	11.1231(6)	-	-	-	-	-	-

[1] - problems with aliasing, [2] - close to the detection limit

Sienkiewicz to include new opacity and EOS data -both from the OPAL project (Iglesias & Rogers 1996, Rogers, Swenson & Iglesias 1996, respectively) - mean effect of rotation, and overshooting. Oscillation properties were calculated with modernized version of Dziembowski's (1977) code, which includes effects of rotation.

Our default hypothesis is that stellar structure is adequately described by standard stellar models, that is that there is no imprints of mass exchange or merging in their current structure. When discussing individual objects we ask whether the data are consistent with this hypothesis. The test is possible if we have a plausible identification of at least one peak in the oscillation spectra with a radial mode. If a measured period is found longer than that of fundamental mode in the model consistent with the star position in the H-R diagram and this position also excludes driving of g-modes, then we may suspect that the object has lower mass than implied by its luminosity.

We consider interpretation of three close frequencies in terms of rotational splitting of $\ell = 1$ mode frequencies. The self-consistency of the hypothesis is checked by comparing the observed and calculated multiplet structures. The frequency distance between the extreme components is a measure of mean rotation rate, which is mode-dependent because different modes probe different parts of the star. The consistency test is possible if nearly uniform rotation is assumed. Then we can evaluate the departure from symmetry induced by higher order effects of rotation and compare the result with observations.

Even if we cannot identify individual peaks in oscillation spectra, still we can compare the frequency ranges where the peaks occur with the range of unstable modes in the models. This is of interest because the presence of oscillations left of the blue edge may indicate a substantial helium enhancement, which is expected in certain models of BSS formation.

Peaks at frequencies much lower than that of the fundamental radial mode are of our interest too. These could be attributed to high order g-modes. It is now a debated problem whether such modes may be excited in δ Scuti stars (Handler 1999, Breger et al. 2002, Dupret et al. 2004). Even more interesting possibility is that such peaks represent tidally induced changes (Aerts et al. 2002, Handler et al. 2002).

Figure 4 shows evolutionary tracks and positions of SXPS from ω Cen in the color-magnitude diagram. Tracks were calculated with two sets of the chemical composition parameters ($Z = 0.002, X = 0.74$) and ($Z = 0.0002, X = 0.75$). The range of Z values is consistent with metal abundances observed among the stars belonging to the cluster (Rey et el. 2000). The range of masses, which is given in the caption, was chosen to cover the range of stellar $B - V$ and M_V values. The tracks were converted from the $\log T_{\rm eff}$ – $\log L$ to the $(B - V) - M_V$ diagram with the use of Kurucz's (1998) tabular data based on his stellar atmosphere model calculations.

The blue edge was determined by means of our linear stability analysis. In this plot, we chose the first overtone because this mode is most frequently excited in the stars considered. The fundamental mode blue edge is redder by some 0.022 mag in $B-V$ and that of the second overtone is bluer by 0.014 mag relative to the that of the first overtone.

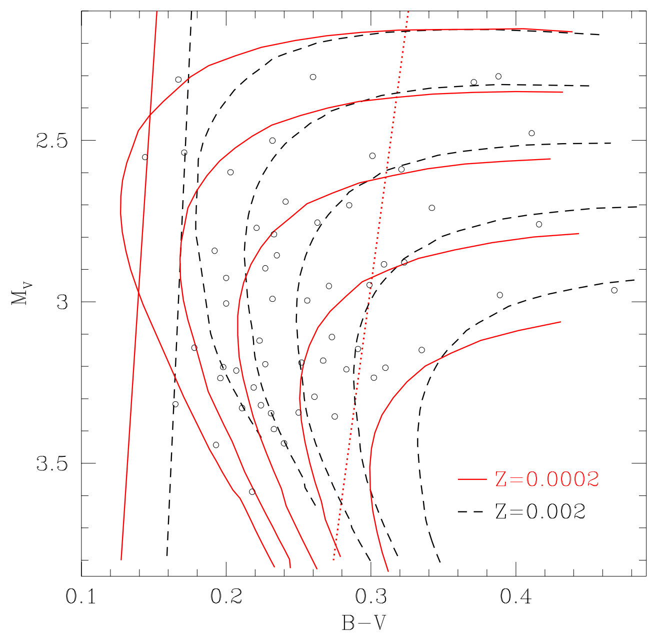

Figure 4. The H-R diagram showing evolutionary tracks in the mass range $1.0 \div 1.2$ with $0.05 M_\odot$ step at $Z = 0.002$ (dashed line) and $0.85 \div 1.05$ at $Z = 0.0002$ (solid line). Straight lines show corresponding positions of the first overtone blue edge. The dotted straight line shows the empirical red edge of the instability strip. Open circle show stellar values taken from Table 1.

These lines depend on mode frequency but not on degree ℓ. The adopted red edge is empirical and based on δ Scuti data (Rodriguez et al. 2000).

We see in Fig. 4 that the blue edge is sensitive to the assumed metal content. Not surprisingly, the sensitivity to helium content is even stronger. After all, it is helium that does most of the mode driving. Increasing the helium abundance from $Y = 0.25$ to 0.50 causes the blueward shift of the first overtone blue edge by 0.05-0.06 mag.

Note that most of our stars fall within the instability strip. However, there are few objects which are redder than the red edge but admittedly their positions are quite uncertain. It may depend on metallicity. There is only one star (NV321, not shown in the plot) which is far bluer than the blue edge but, as we comment in the next section, its colour is very uncertain. Thus, we see no evidence for a substantial helium enhancement in stellar outer layers.

The period-luminosity relations calculated for the first overtone along the tracks are shown in Fig. 5. Similar relations for other radial modes are obtained by the shifts given in the caption. The relations depend on the colour and metal content. Thus, application of SXPS as standard candles seems problematical.

We will use the plots shown in Figs. 4 and 5 to discuss the parameters of individual objects and their mode identification.

Fig. 6 shows the period ratios for consecutive radial mode pairs as functions of the longer period in the pair (hereafter PRP diagram). The relation for the first two radial modes is known as the *Petersen Diagram.* We may see that, just as in the case of double mode Cepheids, the Z-

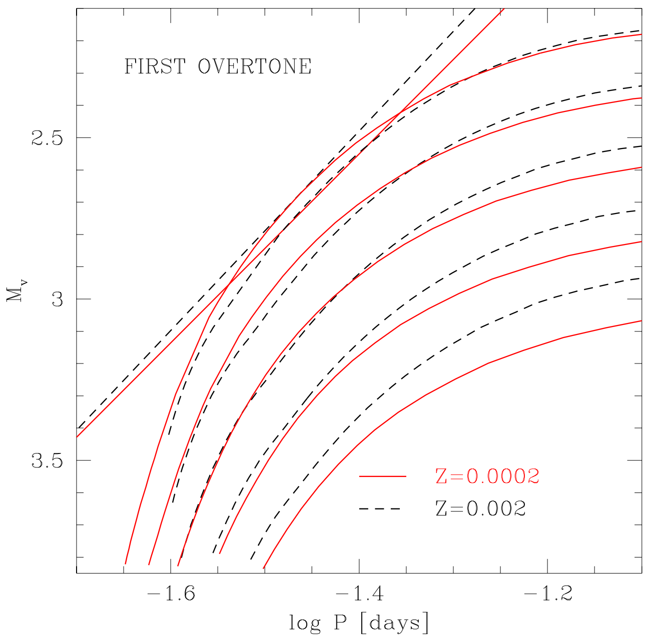

Figure 5. The theoretical period – luminosity relation for the first overtone pulsation and the same models as in Fig. 4. The one for the fundamental mode is shifted by +0.1 and that for the second overtone by -0.08 in log P. Straight lines show corresponding positions of the first overtone blue edge.

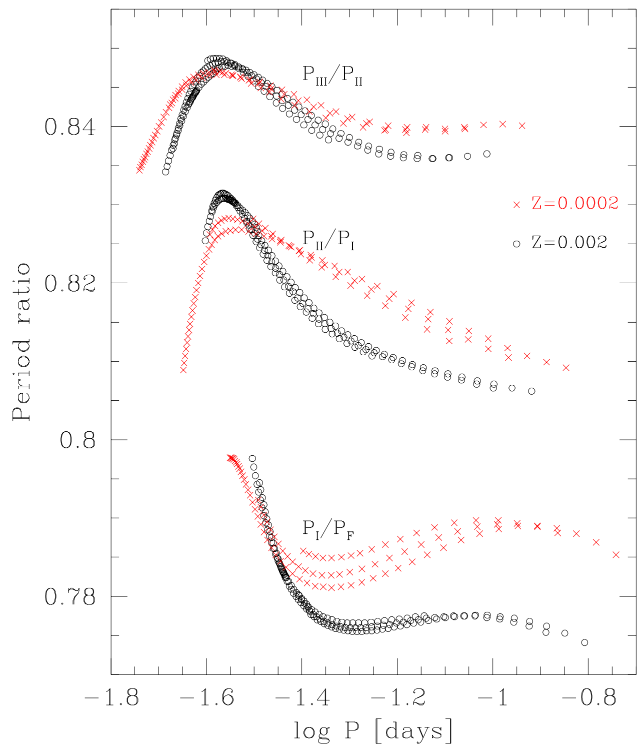

Figure 6. The theoretical period – period ratio diagram for the first four radial modes in our models. On the abscissa we plot the logarithm of the longer period for each pair.

value is important but the pattern of the period–period ratio relation is more complicated.

5 INDIVIDUAL STARS

For each object, the first question we asked is whether any of the peaks in the frequency spectrum could be identified with any of radial modes. Stars with two radial modes exited are of special interest for constraining stellar parameters. With this in mind we first asked wheteher in our sample we find objects with the period ratios that are consistent with the expected values for consecutive radial modes. Fig. 7, which is similar to Fig. 5 of Poretti (2003) for the high amplitude Delta Scuti stars, shows that we have many candidates for two radial mode pulsators. However, since the ranges for each period ratio are rather wide, we cannot use Fig. 7 alone as a tool for a definite mode identification. The witdh of the band for the specfic period ratio arises from the uncertainty in metal abundance, in mass and in the effective temperature. How these parameters affect the period shows is shown in Fig. 6. Thus, both figures must be used jointly.

The agreement with the model values was regarded as a hint. If none of the period pairs gave the ratio consistent with the values seen in the PRP diagram, we concluded that at most only one peak in the oscillation spectrum may be associated with a radial mode. The case of high amplitude pulsation was considered as another hint for the radial mode identification. It was then checked using the position of the star in the H-R and PL diagrams. If there were no high amplitude peaks, we checked only whether frequency of any of the peak in the power spectrum agrees with any frequency of an unstable radial mode (or its close nonradial neighbour) in the model.

V65: The first SXPS found in the field of ω Cen. It is out of our interest because it does not belong to the cluster physically. The variable V65 is the star number 60026 in the proper motion study of van Leeuwen et al. (2000). The probability of membership for this variable is 0%.

V194: This is a very high amplitude pulsator (amp = 0.51 mag). Positions of f_0 and f_1 modes on the PRP diagram (Fig. 6) show that these could be radial fundamental and first overtone modes. According to the standard models the Z value would be intermediate between 0.002 and 0.0002. Then the mass would be close to 1.05 $M_\odot$ according to its position in the H-R and PL diagrams. Its evolutionary status would be near the end of core hydrogen burning. The remaining peaks could be identified only with nonradial modes. We emphasize that high frequency peak f_2 is still within the calculated instability range.

V195: This is another high amplitude pulsator (amp = 0.38 mag). The shape of the light curve suggests the fundamental radial mode identification. Assuming standard evolutionary model, the implied mass is close to 0.95 $M_\odot$ if $Z = 0.0002$ and close to 1.10 $M_\odot$ if $Z = 0.002$. The two close peaks around the dominant frequency are reminiscent of the pattern seen in Blazhko RR*ab* stars.

V197: There are three possible explanations of the frequency pattern found in V197. First, the ratio between f_0 and f_3 frequencies is 0.781 which may indicate that they correspond to the radial fundamenal and first overtone modes. But the star is too red for this hypothesis. The second pos-

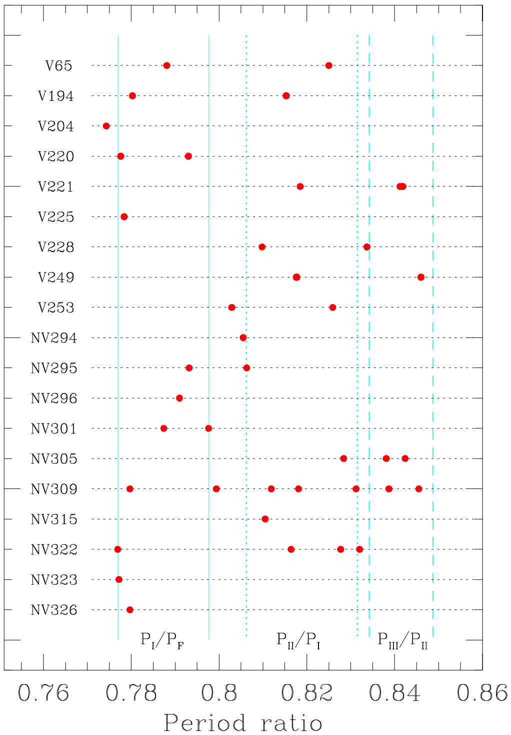

Figure 7. Selected period ratios for multiperiodic stars from Table 1, which may fit the radial oscillations. Vertical lines indicate the ranges of the theoretical period ratios for the first four radial modes in our models, see Fig. 6.

sibility is that only one of three highest peaks might correspond to the radial mode and it could be only the second overtone and then the implied mass would be around 0.9 $M_{\odot}$ and Z should be low. The two peaks close to the main frequency may only be identified as nonradial modes. And alternatively, the three modes might be interpreted as an $\ell = 1$ triplet. Then the rotational period would be around 12 days and rotational velocity would be about 10 km/s.

V198: The mean parameters are inconsistent with the value of period. At this high temperature the period corresponds to a high order g-mode which could not be excited. Perhaps it is a low mass object. However, the color estimate is very uncertain in this case (the error in $B - V$ is about 0.1 mag).

V199: The highest amplitude SXPS in ω Cen. No other significant frequencies were detected at the level above 0.005 mag. Undoubtedly, we see a fundamental mode pulsator. The implied mass must be about 1.0 $M_{\odot}$ and the metallicity must be low.

V200: The shape of the light curve points to the fundamental radial mode identification. The second peak is significantly lower, too low to consider the star as a classical double-mode pulsator. The period ratio of 0.761 could be consistent with the first overtone interpretation of f_1 only if the metallicity is much higher than that considered for stars of ω Centauri. Another problem is too high luminosity for the period. Perhaps the object is a foreground Galactic star.

V204: A high amplitude double-mode pulsator with period ratio equal to 0.774 which indicates metallicity $Z =$ 0.002. Adopting standard models, we get from the H-R and PL diagrams the mass of 1.15 $M_{\odot}$ and the shell hydrogen burning evolutionary status.

V217: A monoperiodic and intermediate amplitude SXPS. In the standard model with low metallicity and mass around 0.90 $M_{\odot}$ the frequency corresponds to the first overtone of radial pulsation or nearby nonradial mode.

V218: The period ratio between two dominant modes falls into the range of the 3rd to 2nd radial overtones ratio. However, for standard models, this identification is inconsistent with the position in the H-R and PL diagrams, which indicates that f_0 could be only the fundamental or a nearby nonradial mode. Such an identification implies mass range $0.95 \div 1.00$ $M_{\odot}$ and Z around 0.0002. Another possibility is that the star is significantly undermassive.

V219: The power spectrum of the star is very much like that of a typical main sequence δ Scuti star, that is, there are many low amplitude peaks spread over wide range of frequencies. Such spectra are extremely difficult to interpret. The main frequency is consistent with fundamental radial mode identification if the metallicity is low and the mass is around 1.00 $M_{\odot}$. The star position in the H-R diagram is near ZAMS, which indicates that the star could be a recent merger of two stars of comparable mass. The low frequency $f_3 = 3.28$ c/d is troublesome. Definitely too low for p-modes. The star is unlikely to excite g-modes, such as seen in γ Doradus stars, because it is one of the hottest in our sample. Perhaps we see ellipsoidal light variations. This is an interesting possibility with ramifications to the problem of BSS origin. The implied orbital period of 0.609 d would be significantly shorter than any of the BSS in the Preston and Sneden (2000) list.

V220: A moderate amplitude multimode pulsator with period ratio between two dominant frequencies equal to 0.778. It implies metallicity close to $Z = 0.002$, which is also consistent with the position of the star in the H-R and PL diagrams and leads to mass estimate of 1.10 $M_{\odot}$. There is a close neighbour of the *bona fide* 1st overtone and it may be interpreted only in terms of nonradial modes.

V221: Many low amplitude peaks, none two of them may be interpreted as two radial modes. High frequencies combined with M_V value indicate excitation of high order p-modes.

V225: A high amplitude pulsator (amp = 0.22 mag) with period ratio between two dominant frequencies equal to 0.778. It implies metallicity close to $Z = 0.002$, which is also consistent with the position of the star at the H-R and PL diagrams and leads to mass estimate of 1.15 $M_{\odot}$. There is a close neighbour of the 1st overtone candidate which could be interpreted as nonradial mode.

V226: A high amplitude pulsator (amp = 0.17 mag). Frequency $f_0 = 26.4185$ c/d may correspond to the first overtone, if the metallicity is rather high and the mass is around 1.05 $M_{\odot}$. Then the frequencies f_1 and f_3 close to f_0 could be associated with nonradial modes. The frequency f_2 is too low to correspond to a nonradial mode located in the neighborhood of the radial fundamental mode; therefore, it could be one of the pure g-modes.

V227: Frequency $f_0 = 26.1605$ c/d may correspond to the first overtone according to the positions of the star in the H-R and PL diagrams. The implied mass estimate is 1.1 $M_{\odot}$ and the metallicity around $Z = 0.002$. Frequencies f_1

and f_2 could be nonradial modes in the vicinity of the first overtone radial mode.

V228: A moderate amplitude multimode pulsator with period ratio between the frequencies f_0 and f_3 equal to 0.834. Looking at the PRP diagram one can find that they can be the first and second overtone radial modes but only in the case of low metallicity. The frequencies f_1 and f_2 correspond then to nonradial modes in the vicinity of the first overtone. Position of the star on the H-R and PL diagrams agrees with assumption of a low metallicity and indicates the mass of 0.90 $M_{\odot}$.

V229: It is one of the bluest SXPS in our sample, much bluer than Kaluzny et al. (1996) found. Since they relay on $V - I$ colours, we checked the object carefully for blending effects and found none. Our colour implies that the dominant period is too long to correspond to the fundamental mode. The problem which is similar to the cases of V198 and V226, where we do not expect excitation of pure g-modes in so hot star.

V231: The dominant frequency $f_0 = 26.6778$ c/d could be due to the radial fundamental mode only for $Z = 0.0002$. In this case, the mass of the star is between 0.95 and 1.00 $M_{\odot}$. The frequencies f_1 and f_2 could be due the excitation of two nearby nonradial modes. The frequency $f_3 = 36.6960$ c/d is associated with nonradial mode placed between the first and the second overtone.

V233: The dominant frequency $f_0 = 27.3691$ c/d could be due to the radial first overtone mode only if $Z \approx 0.0002$. In this case, the mass of the star would be around 0.95 $M_{\odot}$. The low frequency peak at $f_1 = 2.9205$ c/d could indicate that the star is, along with V219, a candidate for an ellipsoidal variable.

V237: The high amplitude (0.27 mag) peak at $f_0 = 15.2433$ c/d could be identified as the radial fundamental mode. Such an identification is consistent with the positions in the H-R and PL diagrams for low Z models. Then the mass of the star is about 0.95 $M_{\odot}$. If f_0 is indeed the fundamental mode then the expected position of the second overtone radial mode is around 24 c/d. Thus, we conclude that the frequency $f_1 = 24.1162$ c/d could correspond to the second overtone. The peak at $f_2 = 15.2013$ c/d is due to a nonradial mode in the vicinity of fundamental frequency.

V238: Again, the dominant frequency $f_0 = 24.5096$ c/d could be due to the excitation of the radial fundamental mode only if Z is low and the mass of the star is 0.95 $M_{\odot}$. The frequencies f_1, f_2 and f_3 may be attributed to nearby nonradial modes. The expected position of the second overtone radial mode is around 38 c/d thus the frequency $f_4 = 39.5205$ c/d would be due to the nonradial p-mode.

V249: A moderate amplitude multimode pulsator with the period ratio between two dominant frequencies equal to 0.818. It is consistent with an assumption that f_0 and f_1 correspond to the first and second overtone radial modes. This requires high Z values, somewhat higher than $Z = 0.002$. However this interpretation is inconsistent with the star position in the H-R and PL diagrams.

V250: A double mode pulsator with f_0 and f_1 being the radial fundamental and the second overtone modes, respectively. The position at the H-R and PL diagrams indicates a low metallicity and the mass between 0.90 and 0.95 $M_{\odot}$.

V252: A monoperiodic and low amplitude star. The position of the star in the H-R and PL diagrams is consistent with the fundamental radial mode identification only for a low metallicity and the mass between 0.85 and 0.90 $M_{\odot}$.

V253: A moderate amplitude multimode pulsator. The dominant frequency could be the fundamental radial mode only for our low metallicity models. In this case, the star has mass around 1.00 $M_{\odot}$. The frequency f_1 corresponds to a nonradial mode in the vicinity of fundamental peak and frequencies f_2 and f_3 to some high order nonradial p modes.

NV294: This is the shortest period SXPS known. Up to now, the shortest period variable of this type was V10 from NGC6397 (Kaluzny and Thompson 2003). NV294 is a multimode and very low amplitude object. With our H-R and PL diagrams the frequency $f_1 = 28.9864$ c/d may be associated with the radial fundamental mode, in a model of high metallicity and mass around 1.2 $M_{\odot}$. In this picture, the frequencies f_0, f_2 and f_3 correspond to the high order nonradial p-modes.

NV295: This is another very short period, low amplitude and multimode object. The frequency $f_1 = 28.3558$ c/d could correspond to the radial second overtone mode but only for low values of Z. In this case, the position of the star at the H-R and PL diagrams indicates the mass between 0.90 and 0.95 $M_{\odot}$. The frequencies f_0, f_2 and f_3 could correspond to nonradial modes.

NV296: Another object similar to NV294 and NV295. There are five frequencies present in the light curve of the star. With our models only the lowest amplitude peak at frequency f_4 might be identified with a radial mode. It would be the second overtone and in this case the metallicity of the star would be around $Z = 0.002$ and the mass would be between 1.10 and 1.15 $M_{\odot}$. In such a case, other frequencies would correspond to nonradial high order p-modes.

NV297: A low amplitude multimode object with four relatively close peaks. One of them could be identified with the second overtone radial mode and then the star mass would be around 1.20 $M_{\odot}$ at $Z = 0.002$ and about 1.05 $M_{\odot}$ at $Z = 0.0002$. We consider possibility that three of the four frequencies represent a rotationally splitted $\ell = 1$ triplet. In the plausible interpretation f_1 would be a retrograde and f_3 would be the prograde mode. Then the frequency separation would imply rather fast rotation (over 100 km/s). However, the calculated position of the $m = 0$ component does not agree with the position of any of the two remaining peaks. It was much closer to the f_3.

NV298: The dominant peak of the two observed in the star may be identified, in our models, with the fundamental radial mode if the metallicity is rather high and the mass is between 1.15 and 1.20 $M_{\odot}$. The second close frequency must then be associated with a nonradial mode.

NV299: The dominant peak could be the radial first overtone mode in a star of a relatively high metallicity and mass around 1.05 $M_{\odot}$. Then the frequency f_1 would correspond to a nonradial mode located between the radial first and second overtones. The star is slightly too red for this interpretation but it is located in a crowded region of the cluster and its V magnitude zero point is determined with the accuracy of around 0.04 mag. Thus the star may be in fact even 0.05 mag bluer.

NV300: A monoperiodic and low amplitude SXPS. The star could be the radial fundamental mode pulsator only if we assume the high metallicity and the mass of around 1.15 $M_{\odot}$.

NV301: A multimode and low amplitude SXPS. One of the two dominant frequencies may be the radial second overtone mode, according to our models. The star has then a high metallicity and the mass around 1.05 $M_{\odot}$. The frequencies f_2 and f_3 should correspond to the high order nonradial p-modes.

NV302: A monoperiodic and low amplitude star. The frequency $f_0 = 28.1538$ c/d could be the first overtone radial mode but only for our $Z = 0.002$ models. In this case, the mass of the star is between 1.10 and 1.15 $M_{\odot}$. It is also possible that f_0 is the second overtone. This requires low Z and, in this case, the mass of the star is between 0.90 and 0.95 $M_{\odot}$.

NV303: A monoperiodic and very low amplitude star. The only frequency determined could be associated with the first radial overtone. Then the star has low metallicity and mass slightly less than 1.0 $M_{\odot}$.

NV304: A similar pulsator to NV303. Again, the first radial overtone interpretation possible, however in this case the models imply high metallicity and mass around 1.05 $M_{\odot}$.

NV305: A multiperiodic object with interesting power spectrum. The amplitude increases systematically with the frequency. The period ratio between two dominant peaks is equal to 0.828 - a value which could be the ratio between the first and second radial overtones, but only for very low metallicity. It is supported by the position of the star in the H-R and PL diagrams implying the mass in range of $0.85 \div 0.90$ $M_{\odot}$. The frequencies f_2 and f_3 would correspond to nonradial peaks in the vicinity of the fundamental radial mode.

NV306: One of the faintest SXPS in our sample. The dominant frequency could be due to the radial fundamental mode. With this interpretation, the metallicity of the object is low and its mass is between 0.90 and 0.95 $M_{\odot}$. The expected position of the second overtone radial mode is close to 40 c/d, thus the second peak could be connected with this mode.

NV307: A monoperiodic and moderate amplitude star. Our models imply that the excited mode must be of higher order than two, which seems to be in conflict with the star relatively low temperature.

NV308: A multiperiodic object. Of the three dominant peaks at low frequency one could be identified with the first overtone for our low metallicity models with the mass of about 0.90 $M_{\odot}$. We also considered the possible interpretation of these three peaks in terms of rotationally splitted $\ell = 1$ mode. In this case, the problem is opposite to that accounted in NV297 - the observed asymmetry is too high for the rotation rate of about 50 km/s implied by the distance between f_0 and f_1.

NV309: The star has one of the richest frequency spectrum. We determined as many as seven frequencies. The f_5/f_1 ratio could be the frequency ratio between the first and second overtones of radial pulsations. This interpretation is however in conflict with the H-R position, where the star is too red. For this star we obtained a consistent interpretation of three peaks (f_5, f_0 and f_3) as a rotational splitted $\ell = 1$ triplet. For our model with $Z = 0.0002$ and mass of 0.95 $M_{\odot}$ the separation between f_3 and f_5 implies rotational velocity of 60 km/s. With this velocity the centroid component, displaced from the center by the second order effect of rotation, comes close to f_0. This triplet is not far from the frequency of the first radial overtone. The peak f_4 would then be located in the vicinity of the second overtone while the highest frequency peaks (f_2 and f_1) of the third overtone.

NV310: The only two frequencies are close to the expected position of the radial second overtone, for our models with high metallicity and mass around 1.10 $M_{\odot}$.

NV311: The two frequencies measured in this star, $f_0 = 24.1469$ c/d and $f_1 = 36.6940$ c/d, may be due to the radial fundamental and the second overtone modes, respectively. Unfortunately, we can not verify this hypothesis because we do not know the exact magnitude and color of the star, which is located in very crowded region of the cluster.

NV312: One of the brightest SXPS in ω Cen. The frequency $f_0 = 23.0802$ c/d could be associated with the radial second overtone mode but only for high metallicity. In this case, the mass of the star is around 1.2 $M_{\odot}$. The peak at $f_1 = 36.8$ c/d can be interpreted as the high order p-mode.

NV313: A monoperiodic, high amplitude and faintest SXPS in the field of ω Cen. The high amplitude may suggest that the star is a radial mode pulsator. The problem is that in our standard models, the star with the observed effective temperature and luminosity would have the fundamental radial mode period by factor 1.3 shorter. The star is also one of the hottest in our sample and we certainly do not expect excitation of g-modes in such a star. In fact, we would rather expect higher order modes excitation, therefore this object is likely to be undermassive by factor of 1.7 or more.

NV314: The frequencies $f_0 = 23.7405$ c/d and $f_2 = 36.4036$ c/d could be the radial fundamental and second overtone modes, respectively, but only if the star would be bluer by 0.06 mag. It is possible, because the star is located in the crowded region (three bright companions) and zero point in V-band is poorly determined.

NV315: One of the brightest SXPS in ω Cen with a rich oscillation spectrum. The photometric data combined with our model parameters imply that even the lowest frequency, f_0, is higher than the second overtone radial mode. The preference to the high frequency mode excitation seems to be in conflict with the low temperature of the star, the one of the lowest in our sample.

NV316: A monoperiodic and low amplitude star. The period is too long for fundamental radial mode, according to our models. Perhaps the star is another case of an undermassive object.

NV317: A low amplitude multiperiodic star. Assuming our standard models, the frequency $f_0 = 23.4525$ c/d could be attributed to the radial second overtone mode in a star with a rather high metallicity and mass of around 1.05 $M_{\odot}$. Three other peaks (f_1, f_3 and f_2) in this model can be interpreted as a rotationally splitted $\ell = 1$ triplet, which implies rotational velocity of about 120 km/s. Alternatively, another combination of three peaks (f_0, f_3 and f_2) might be interpreted as an $\ell = 1$ triplet, which would imply rotational velocity of about 80 km/s.

NV318: A low amplitude and monoperiodic star. The frequency f_0 could be due to the radial second overtone mode in a model with high metallicity and mass between 1.05 and 1.10 $M_{\odot}$.

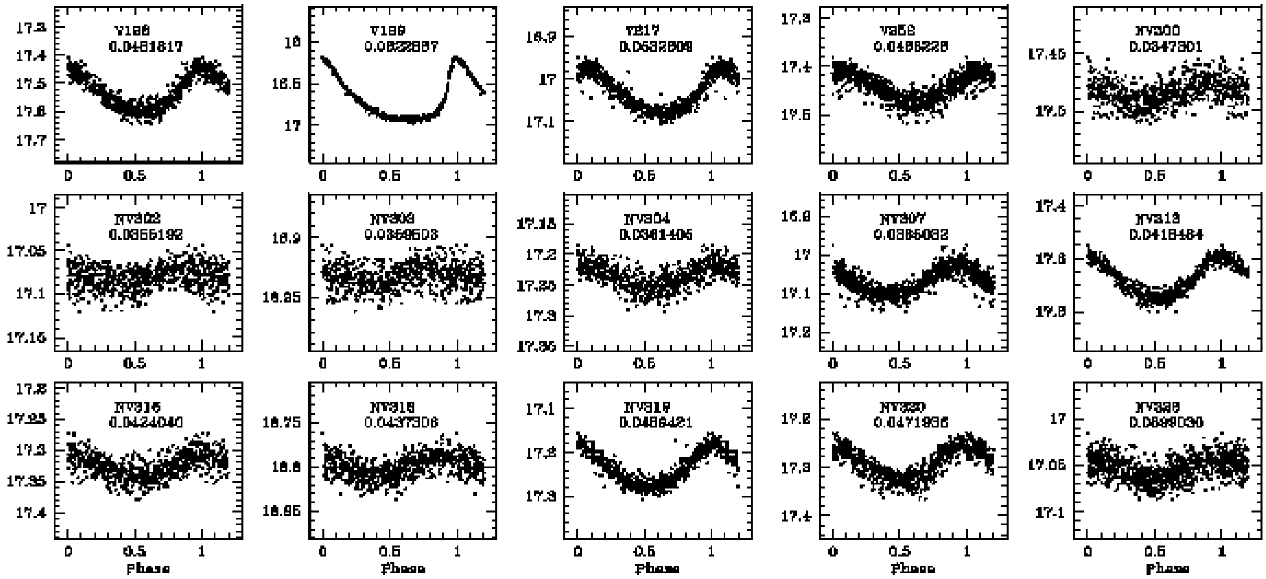

Figure 8. Phased light curves of monoperiodic SXPS in ω Centauri

NV319: A moderate amplitude and monoperiodic star. The only frequency could be that of the radial first overtone mode in a star of low metallicity and the mass between 0.85 and 0.90 $M_{\odot}$.

NV320: It is almost identical to the previous object.

NV321: A multiperiodic and moderate amplitude star. The frequencies f_0, f_1 and f_2 form an asymmetric triplet which perhaps might be interpreted as rotationally splitted $\ell = 1$ mode. Unfortunately, the variable is located in very crowded field and the mean B and V magnitudes are very uncertain.

NV322: A moderate amplitude variable with one of the richest power spectrum. The ratio between two dominant frequencies is 0.777 which may suggest that they are fundamental and first overtone radial modes. We have no color determination for this star and we can not exploit this hypothesis.

NV323: A double mode and low amplitude pulsator. Surprisingly, we found the same period ratio of 0.777 as in previous case. However, we have a problem with interpretation of the frequencies in terms of the fundamental and first overtone radial pulsations. The period ratio suggests the metallicity of $Z \approx 0.002$. Our models imply the H-R position by some of 0.06 mag bluer than observed.

NV324: A high amplitude and multiperiodic star. Its rich power spectrum is shown in Fig. 2. According to our models, the dominant frequency is close to the radial first overtone for low metallicity and mass of around 1.05 $M_{\odot}$. The frequencies f_1, f_2 and f_5 are all close to that of the third radial overtone mode.

NV325: A moderate amplitude and multiperiodic object. The dominant frequency may be interpreted, according to our models, as due to the second radial overtone in a star with mass between 1.15 and 1.20 $M_{\odot}$ if $Z = 0.002$ or between 1.00 and 1.05 $M_{\odot}$ if $Z = 0.0002$. Presence of three high frequency modes is surprising in view of rather low temperature and high luminosity of the object.

NV326: This is a classical double mode star with $f_0 = 17.5728$ c/d as radial fundamental and $f_1 = 22.5375$ c/d as the first overtone modes. The frequency ratio of 0.780 nicely agrees with that of fundamental and first overtone in an intermediate metallicity object. Further, the periods and the metallicity agree with the position of the star in the H-R and PL diagrams. The implied mass is then between 0.95 and 1.00 $M_{\odot}$.

NV327: It is one of the bluest stars in our sample. The frequency f_0 may be associated with the fundamental mode but only if the star is significantly undermassive.

NV328: A low amplitude and monoperiodic star. It is the reddest star in our sample. The only frequency, according to our models, may be interpreted as the fundamental radial mode, implying the mass around 1.00 $M_{\odot}$ at $Z = 0.0002$ or mass between 0.85 and 0.90 $M_{\odot}$ at $Z = 0.002$.

6 CONCLUSIONS

In most cases the observed properties of SXPS in ω Centauri may be explained in terms of standard evolutionary models and their linear nonadiabatic properties. In a number of cases, where the observational evidences pointed to radial mode excitation, we derived the masses of the objects. They all fall into the range $0.90 \div 1.15 M_{\odot}$. The implied evolutionary status covers both the main sequence and early post-main sequence evolutionary phases.

Only in four cases the observed parameters were inconsistent with the standard models and could be reconciled with the undermassive objects. Such objects could arise in several situations. They can appear as a result of mergers, if there is a mass loss or element mixing. They could also arise as the result of mass exchange in binary systems. This possibility may be contemplated only in the case of very large mass loss on the lower red giant branch. Applicable models would have rather low mass ($\sim 0.2 M_{\odot}$), most of which contained in the helium core. Such models were once considered by Dziembowski and Kozłowski (1974) for high amplitude δ Scuti stars, called then Dwarf Cepheids.

We found two cases of stars with long periodicities that may be interpreted as due to the tidally induced distortion. This could be an indirect evidence for binarity. Possible implications for the mechanism of BSS formation are interesting. Therefore, the two objects deserve further studies to check the interpretation. This could be done by searching for induced pulsation period changes (current data do not allow to reject nor confirm the proposal) or by means of radial velocity measurements.

Our search for rotationally split triplets resulted in three plausible cases. For NV309 the inferred equatorial velocity would be about 60 km/s, and for NV317 it would be about 80 or 120 km/s, depending on three frequency peaks involved. For V197 the interpretation of all three close peaks as $\ell = 1$ triplet results in equatorial rotational velocity of about 10 km/s.

We found considerable diversity in pulsational behaviour ranging from that typical for main sequence δ Scuti stars characterized by low amplitude and multimode variability to high amplitude Cepheid-like monomode pulsations. This is quite amazing bearing in mind the fact that the spread in V brightness is only about one magnitude. To give the picture of the observed diversity, Fig. 8 shows the phased light curves of the monoperiodic pulsators from our sample.

Examples of δ Scuti-like behaviour are objects like V219, NV294, NV295 and NV296. These are among the faintest and the hottest stars in our sample. Amongst the faintest objects there are also some relatively high amplitude pulsators (V198, V249 and NV313) but all of them are suspected for being undermassive.

The star V199, whose light curve resembles those of Cepheids or RR*ab* stars, is amongst most luminous objects. Other high amplitude objects are multiperiodic. Among them there are five classical double mode pulsators i.e. stars with fundamental and the first overtone excited. These objects were crucial for deriving constrains on masses and metallicities. In three of them we detected additional, apparently nonradial modes. Coexistence of high amplitude radial modes with low amplitude nonradial modes was first seen by Walraven, Walraven and Balona (1992) in the δ Scuti star AI Vel (see also Poretti 2003). In some of our cases the nonradial modes are located close to radial modes in the frequency spectrum but not in all, just like in AI Vel.

Three clean cases of spectra consisting of a dominant peak surrounded by close low amplitude peaks are V195, V197 and NV321. These are possible analogs of Blazhko RR*ab* stars.

ACKNOWLEDGMENTS

We are thankful to Dr. Poretti, the referee, for pointing misidentification of $f_0 + f_1$ frequency in NV324. This work was supported by the KBN grants number 1 P03D 006 27 to A. Olech, 5 P03D 030 20 to W.A. Dziembowski, 5 P03D 012 20 to A.A. Pamyatnykh, and 5 P03D 004 21 to J. Kaluzny. A. Schwarzenberg-Czerny would like to acknowledge generous grant by Clifford and Mary Corbridge Trust of Cambridge, England.

REFERENCES

Aerts C., Handler G., Arentoft T., Vandenbussche B., Medupe R., Sterken C. 2002, MNRAS, 333, L35
Breger M. et al. 2002, MNRAS, 329, 531
Carney B.W., Latham D.W., Laird J.B., Grant C.E., Morse J.A., 2001, AJ, 122, 3419
Dupret M.-A., Grigahcéne A., Garrido R., Gabriel M., Scuflaire R. 2004, A&A, 414, L1
Dziembowski, W. & Kozłowski, 1974, Acta Astron., 24, 245.
Dziembowski W., 1977, Acta Astron., 27, 203
Eadie W.T., Drijard D., James F.E., 1971, Statistical methods in experimental physics, Amsterdam, North-Holland.
Ferraz-Mello, S., 1981, AJ, 86, 619
Foster, G., 194, AJ, 109, 1889
Gray D. F. & Desikachary K., 1973, ApJ 181, 523.
Handler G. 1999, MNRAS, 309, L19
Handler G. et al. 2002, MNRAS, 333, 262
Iglesias C.A., Rogers F.J. 1996, ApJ, 464, 943
Kaluzny J., Kubiak M., Szymański M., Udalski A., Krzemiński W., & Mateo M. 1996, A&AS, 120, 139
Kaluzny J., Kubiak M., Szymański M., Udalski A., Krzemiński W., & Mateo M., 1997a, A&AS, 122, 471
Kaluzny J., Thompson I.B., Krzemiński W., Olech A., Pych W., Mochejska B., 2002, in van Leeuwen F., Hughes J.D., Piotto G., eds., ASP Conf. Ser. Vol. 265, "Omega Centauri, A Unique Window into Astrophysics", Astron. Soc. Pac., San Francisco, p. 155
Kaluzny J., Thompson I.B., 2003, AJ, 125, 2534
Kaluzny J., Olech A., Thompson I.B., Pych W., Krzemiński W., Schwarzenberg-Czerny A., 2004, A&A, 424, 1101
Lomb, 1976, A&SS 39, 477
Lombardi J.C., Jr., Rasio F.A., 2002, in Shara M.M. ed., ASP Conference Proceedings, Vol. 263, "Stellar Collisions, Mergers and their Consequences", San Francisco: Astronomical Society of the Pacific, p. 35
Lombardi J.C., Warren J.S., Rasio F.A., Silla A., Warren A.R., 2002, ApJ, 568, 939
Kepler, S.O., 1993, in proceedings of Second WET Workshop, Baltic Astronomy, 2, 515
Kurucz R.L., 1998, in Bedding T.R., Booth A.J., Davis J. eds., Proceedings of IAU Symposium 189, "The Interaction between Observation and Theory", Kluwer, Dordrecht, p. 217
Mazur B., Krzemiński W., Thompson I.B., 2003, MNRAS, 340, 1205
McCrea W.H., 1964, MNRAS, 128, 147
Paczyński B., 1970, Acta Astron., 20, 47
Poretti E., 2003, A&A, 409, 1031
Pych W., Kaluzny J., Krzemiński W. Schwarzenberg-Czerny A., Thompson, I. B., 2001, A&A, 367, 148
Rey S.-C., Lee Y.-W., Joo J.-M., Walker A., Baird S., 2000, AJ, 119, 1824
Rodriguez E., López-González M.J., López de Coca P., 2000, in Breger M., Montgomery M.H., eds., ASP Conf. Ser. Vol. 210, "Delta Scuti and Related Stars", Astron. Soc. Pac., San Francisco, p. 499
Rogers F.J., Swenson F.J., Iglesias C.A. 1996, ApJ, 456, 902
Scargle, J.H., 1982, ApJ, 263, 835
Schlegel D.J., Finkbeiner D.P., Davis M. 1998, ApJ, 500, 525
Schwarzenberg-Czerny A., 1996, ApJ Letters, 460, L107

Schwarzenberg-Czerny A., 1999, ApJ, 516, 315
Thompson I.B., Kaluzny J., Pych W., Burley G., Krzemiński W., Paczyński B., Persson S.E., Preston G.W., 2001, AJ, 121, 3089
van Leeuwen F., Le Poole R.S., Reijns R.A., Freeman K.C., de Zeeuw P.T. 2000, A&A, 360, 472
Walraven Th., Walraven J., Balona L.A., 1992, MNRAS, 254, 59